

## Neutralized wettability effect of superhydrophilic Cr-layered surface on pool boiling critical heat flux

Hong Hyun Son, Uiju Jeong, Gwang Hyeok Seo, Gyoodong Jeun, Sung Joong Kim\*

Department of Nuclear Engineering, Hanyang University

222 Wangsimri-ro, Seongdong-gu, Seoul 04763, Republic of Korea

hhson@hanyang.ac.kr, uijeong@hanyang.ac.kr, seokh@hanyang.ac.kr, thlab@hanyang.ac.kr,

\*Corresponding author: sungkim@hanyang.ac.kr

### 1. Introduction

The design requirement for the accident-tolerant fuel (ATF) cladding is to reduce potential exothermic oxidation and hydrogen generation dramatically during hypothesized severe core degradation [1]. There are two promising methods to hinder high temperature steam reaction of clad material. First one is to replace a conventional zircaloy clad body with a new accident tolerant cladding and the other is to deposit an additional microlayer on an existing zircaloy-clad surface. The former method is deemed challenging due to longer development period and license issue.

In this regard, FeCrAl, Cr, and SiC have been received positive attention as ATF coating materials because they are highly resistant to high temperature steam reaction causing massive hydrogen generation [1]. In this study, Cr was selected as a target deposition material on the metal substrate because we found that Cr-layered surface becomes superhydrophilic, favorable to delaying the triggering of the critical heat flux (CHF).

Thus in order to investigate the effect of Cr-layered superhydrophilic surfaces (under explored coating conditions) on pool boiling heat transfer, pool boiling experiment was conducted in the saturated deionized water under atmospheric pressure. As a physical vapor deposition (PVD) method, the DC magnetron sputtering technique was introduced to develop Cr-layered nanostructure. As a control variable of DC sputtering, substrate temperature was selected. Surface wettability and nanostructure were analyzed as major surface parameters on the CHF.

### 2. Impact of DC sputtering on change of surface characteristics

#### 2.1 DC sputtering process

As shown in Fig. 1, main components of the DC magnetron sputtering system in vacuum chamber include a target material (selected as Cr in this study) assembled with magnets and a DC gun, a substrate with halogen heaters, and an argon (Ar) injection line. As a typical DC sputtering process, Ar<sup>+</sup> particles ionized by high potential difference are bombard to a target material. Subsequently sputtered atoms (Cr) ejected from the target deposit on the substrate with high energy potential. During continuous sputtering process, adatoms (atoms

physically deposited on the substrate) form individual clusters. Eventually, a thin film layer on the substrate is developed with fine nanostructures.

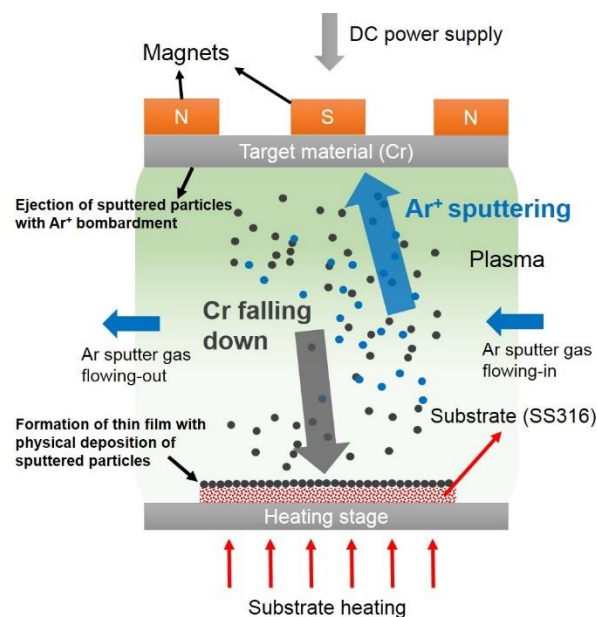


Fig. 1. Schematic of DC magnetron sputtering process.

In typical sputtering process, thickness of thin film and its surface nanostructure vary with substrate temperature, exposure time, and DC power, to mention a few. Since present study focuses on the effect of Cr-layered (or - nanostructured) surface on the performance of boiling heat transfer, we selected substrate temperature as a control variable. Because the formation of nanostructures on the substrate is primarily governed by shadowing, re-emission, and diffusion effects, their operational mechanisms become effective with substrate temperature [2, 3]. For example, higher substrate temperature promotes diffusion process of adatoms over the surface, inducing the formation of dense nanostructures with lower particle size.

Table I shows DC sputtering conditions. Only substrate temperature was controlled at 150 and 600 °C. During 1 hour sputtering, approximately 1 μm thin film was formed for two cases. In addition, through energy dispersive spectrum (EDS) mapping result (Table II), it is confirmed that Cr composition in 1 μm thin film reaches approximately 96 wt.% without any impurities, except for very small amount of oxygen atoms (~3 wt.%).

It exhibits that the thin film consists mainly of Cr-based structures.

Table I: DC sputtering conditions

|                            | Bare | Cr-150°C-1hr       | Cr-600°C-1hr       |
|----------------------------|------|--------------------|--------------------|
| Target material            | -    | Cr                 | Cr                 |
| Substrate temperature (°C) | -    | 150                | 600                |
| Exposure time (hour)       | -    | 1                  | 1                  |
| Working pressure (Torr)    | -    | $1 \times 10^{-2}$ | $1 \times 10^{-2}$ |
| DC power (W)               | -    | 150                | 150                |
| Argon flow rate (sccm)     | -    | 29.7               | 29.7               |

Table II: EDS mapping result (measured in  $15 \times 15 \mu\text{m}^2$  SEM images)

| Test specimen | Composition of major elements (wt.%) |      |     |
|---------------|--------------------------------------|------|-----|
|               | Fe                                   | Cr   | O   |
| Bare*         | 70.9                                 | 14.8 | 1.4 |
| Cr-150°C-1hr  | -                                    | 96.7 | 3.2 |
| Cr-600°C-1hr  | -                                    | 96.9 | 3.0 |

\*Another elements consist of C (1.8wt.%), Si (0.5wt.%), Mo (1.5wt.%), and Ni (8.9wt.%).

## 2.2 Formation of nanostructure and its impact on roughness and wettability changes

In Table III, atomic force microscope (AFM) data are summarized for each surface. Averaged roughness ( $R_a$ ) value is almost the same for all cases, but area ratio ( $A_{\text{ratio}}$ ) is higher in Cr-layered surfaces compared to the bare surface. This indicates that abundant Cr clusters are distributed uniformly along initially-developed surface profile as a form of nanostructure.

Table III: AFM result

| Test specimen | $R_a$ (nm) | $A_{\text{ratio}}$ (-) | Mean value* of phase degree (°) |
|---------------|------------|------------------------|---------------------------------|
| Bare          | 118        | 1.15                   | -18.8                           |
| Cr-150°C-1hr  | 152        | 1.29                   | 10.6                            |
| Cr-600°C-1hr  | 126        | 1.32                   | 11.5                            |

\*This value was averaged in the range of  $10 \times 10 \mu\text{m}^2$ .

It can be also confirmed in 3D roughness image (Fig. 2(a)) and its line profile (Fig. 2(c)). Unlike bare surface, on the Cr-layered surfaces, nano-rough line profile forms mainly on the ridge area.

More significantly, wettability change on the Cr-layered surfaces could be identified by measuring the

phase degree. Phase degree is measured using tapping mode in AFM facility and its signal source is related to energy dissipation from the interaction between oscillating cantilever and the surface. Typically, the brighter area in the phase image (Fig. 2(b)) and higher phase degree (Fig. 2(c)) indicates the more hydrophilic surface. As shown in Table III, Cr-based nanostructures reliably showed a higher mean phase degree of  $10.6^\circ$  for the Cr-150°C-1hr and  $11.5^\circ$  for the Cr-600°C-1hr than  $-18.8^\circ$  in the bare surface.

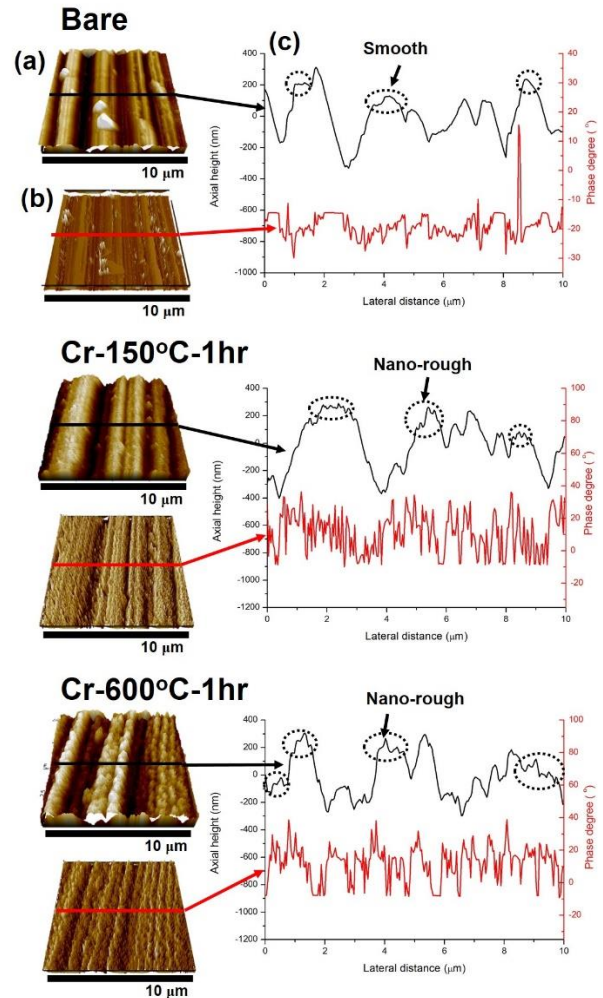


Fig. 2. (a) 3D roughness image, (b) 3D phase image, and (c) their line profiles along the lateral distance of  $10 \mu\text{m}$ .

In addition, phase degree distributes more densely on the Cr-600°C-1hr than in the Cr-150°C-1hr because diffusion effect during sputtering process occurs stronger in the higher substrate temperature. It also implies that hydrophilic Cr-based clusters are more densely-distributed on the Cr-600°C-1hr (particle size  $\sim 150 \text{ nm}$ ) than on the Cr-150°C-1hr (particle size  $\sim 250 \text{ nm}$ ). This result agrees well with micro/nanostructures presented in SEM images (Fig. 3(a, b)) and also Zone model suggested by Thornton [2].

However, the aforementioned difference of Cr-layered surfaces is hardly distinguished in measuring static

contact angle. Because liquid droplets completely spread over the Cr-layered surfaces in a few milliseconds (Fig. 4). So there was an expectation that these surfaces are superhydrophilic favorable to boiling heat transfer.

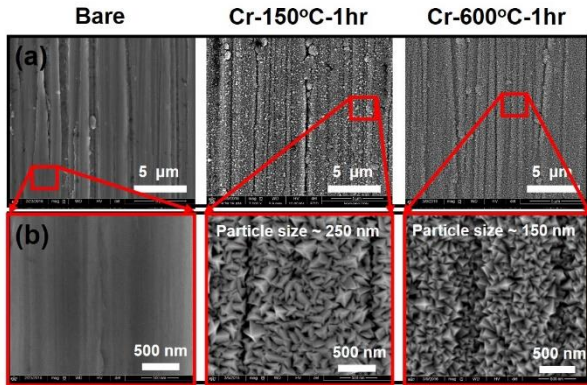


Fig. 3. SEM images of (a) microstructure and (b) nanostructure.

In more detail, wettability of these surfaces was distinguished by tracking spreading history of liquid droplet. As shown in Fig. 4, liquid spreading phenomenon involves rapid angle transition and liquid absorption onto the surface as soon as dropped. Especially below 10°, liquid droplet becomes completely wetted (or absorbed) over the surface. Then, there was no contact line of droplet with the surface. This spreading effect has been investigated by Ahn et al. They distinguished spreading capability on the micro/nano and nano-only structures, observing change of contact angle, precursor lines and remained droplet volume [4]. In their study, micro/nano coupled structure promoted angle transition and extension of precursor line.

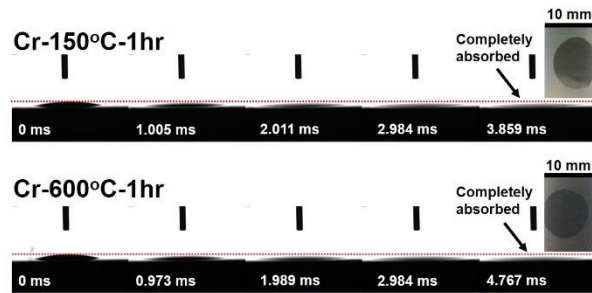


Fig. 4. Spreading history of 5 μl liquid droplet on Cr-layered surfaces at room temperature. In each photograph, shooting timing were measured by Krüss EasyDrop instrument.

However, in our observation (Fig. 4), significant difference in each Cr-layered surface was hardly observed. Angle transition and movement of precursor line were almost the same. Thus, wetting performance at the room temperature was not distinguished regardless of substrate temperature condition.

### 3. Experimental description

As shown in Fig. 5, the test specimen was heated using a DC power supply via copper electrodes connected to each end side of the test specimen. In order to measure the inner surface temperature opposite to the heat transfer surface and voltage drop along the test specimen, a K-type thermocouple and a pair of voltage tap were attached to the end side of the test specimen. The length, width, and thickness of test specimen are 35, 10, and 2 mm, respectively.

The CHF was determined when inner wall temperature jumped rapidly more than 200 °C or voltage drop also increased due to fast oxidation.

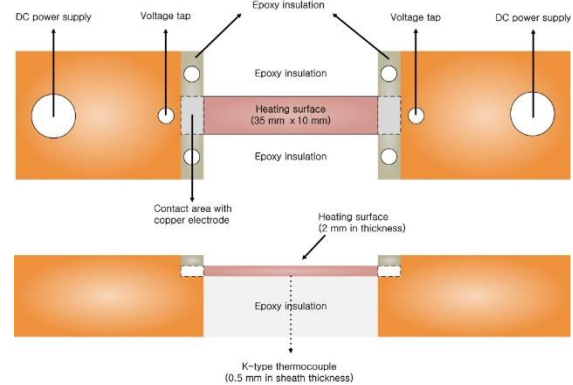


Fig. 5. Schematic of test section.

Applied heat flux was calculated using Joule's equation as shown in Eq. (1).

$$q'' = \frac{Power}{A_{heated}} = \frac{VI}{WL} \quad (1)$$

Here, V is voltage drop at the heating material, I is current, W is width of heat transfer area, L is length of heat transfer area. Using a propagation of error method, measurement uncertainty was estimated as 5.2%.

### 4. Result and discussion

For a few years, the CHF studies focusing on liquid spreading [4] or wicking [5] effects have reported that rewetting and capillary wicking capabilities enhanced by superhydrophilic nature and micro/nano structures effectively hinder the formation of dry patches during fully-developed nucleation, and in turn, delay the triggering of the CHF. This spreading (or hemi-wicking) force has been recognized as an additional contributor to CHF enhancement in Kandlikar's wettability-based CHF model [6].

For the Cr-layered surfaces, liquid spreading was also observed at the room temperature (Fig. 4). However, interestingly, its impact on the CHF was not observed at all in this study. As shown in Fig. 6, CHF values of all explored surfaces rather were close to the CHF of bare

surface, which is well matched with the Zuber's hydrodynamic instability model [7].

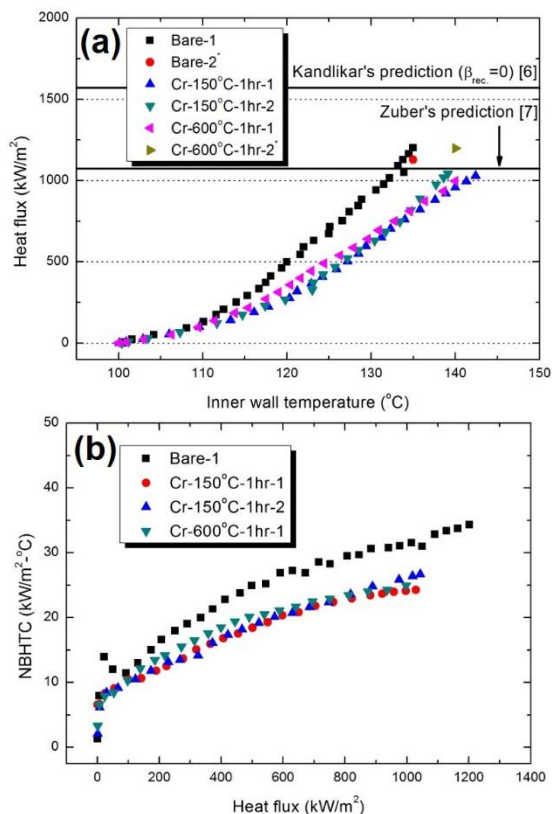


Fig. 6. (a) Boiling curve and (b) change of nucleate boiling heat transfer coefficient according to an increase of heat flux. <sup>®</sup>K-type thermocouples attached to back side of test specimen were malfunctioned.

Present CHF data for superhydrophilic surfaces cannot be explained by existing wettability-based CHF models [4, 5, 6] because there was no CHF enhancement. Recently, experimental evidences have been suggested to argue that wettability alone without other structural bases is not a dominating surface parameter affecting the CHF [8, 9]. These studies strongly pointed out the fact that wettability is effective to the CHF with the existence of abundant nucleation cavities or porous structure having wicking channel. Note that those definition is only applied to horizontally upward-heating condition.

Micro/nano structures on Cr-layered surfaces explored in this study consist of very dense morphology because nanosize (100 ~ 250 nm) fine Cr clusters deposited agglomerate together without any pores. It can also contribute to reduction of the nucleation. More importantly, under superhydrophilic condition, active nucleation seems to be rather suppressed, rarely relieving trapped heat from the heater surface. Accordingly, surface temperature of Cr-layered surfaces increased faster than bare surface (Fig. 6(b)), despite higher roughness and surface area ratio (Table III). Based on this finding, we concluded that effect of superhydrophilic surface with nanostructure of Cr-layer on the pool boiling CHF was neutralized by the reduction of

nucleation sites. As a consequence, this Cr-layered nanostructured surface tends to deteriorate heat transfer coefficient.

## 5. Conclusions

In this study, to enhance thermal margin of ATF clad surface, CHF experiment for Cr-layered surfaces was conducted. Cr-layer was deposited on the metal surface using magnetron DC sputtering technique. However, under explored conditions, CHF enhancement was not observed, despite superhydrophilic characteristic of Cr-layered surfaces. We believe that highly dense micro/nano structure without nucleation cavities and inner pores neutralized the wettability effect on the CHF. Moreover, superhydrophilic surface with deficient cavity density rather hinders active nucleation. This emphasizes the importance of micro/nano structure surface for enhanced boiling heat transfer. Thus, future work should direct to fabricate Cr-layered superhydrophilic surface while having cavities-based microstructure.

## ACKNOWLEDGEMENT

This research was supported by the Basic Science Research Program through the National Research Foundation of Korea (NRF) funded by the Ministry of Science, ICT & Future Planning (No. 2015R1C1A1A01054861)

## REFERENCES

- [1] S. Bragg-Sitton, Development of advanced accident-tolerant fuels for commercial LWRs, Nuclear News, pp. 83-91, 2014.
- [2] J.A. Thornton, Influence of apparatus geometry and deposition conditions on the structure and topography of thick sputtered coatings, Journal of Vacuum Science & Technology, Vol.11, pp. 666-670, 1974.
- [3] J.A. Thornton, The microstructure of sputter-deposited coatings, Journal of Vacuum Science & Technology, Vol. 4, pp. 3059-3065, 1986.
- [4] H.S. Ahn, H.J. Jo, S.H. Kang and M.H. Kim, Effect of liquid spreading due to nano/microstructures on the critical heat flux during pool boiling, Applied Physics Letter, Vol. 98, p. 071908, 2011.
- [5] K.-H. Chu, R. Enright and E.N. Wang, Structured surfaces for enhanced pool boiling heat transfer, Applied Physics Letter, Vol. 100, p. 241603, 2012.
- [6] S.G. Kandlikar, A theoretical model to predict pool boiling CHF incorporating effects of contact angle and orientation, Journal of Heat Transfer ASME, Vol. 123, pp. 1071-1079, 2001.
- [7] N. Zuber, Hydrodynamic aspects of boiling heat transfer (thesis), 1959.
- [8] Y.H. Maeng, S.L. Song and J.Y. Lee, Unaffectedness of improved wettability on critical heat flux enhancement with TiO<sub>2</sub> sputtered surface, Applied Physics Letter, Vol. 108, p. 074101, 2016.
- [9] H. O'Hanley, C. Coyle, J. Buongiorno, T. McKrell, L.-W. Hu, M. Rubner and R. Cohen, Separate effects of surface roughness, wettability, and porosity on the boiling critical heat flux, Applied Physics Letter, Vol. 103, p. 024102, 2013.